ORIGINAL ARTICLE

DOI: https://doi.org/10.18599/grs.2021.1.10 Russian Original 2021. Vol. 23. Is. 1. Pp. 94–105

Typomorphism of rock-forming minerals of Lunar regolith, Luna-16, -20, -24: comparision of sea vs continent vs sea

A.B. Makeyev[1], N.I. Bryanchaninova[2]*

[1]*Institute of Geology of Ore Deposits, Mineralogy, Petrography and Geochemistry of the Russian Academy of Sciences, Moscow, Russian Federation*

[2]*Geological Institute of the Russian Academy of Sciences, Moscow, Russian Federation*

Abstract. The study focuses on the comparison of the chemical and mineral composition of Lunar regolith probes from Luna-16, -20, -24 stations and their the sea-continent environments. Using microprobe JXA-8200 and JSM-5610LV (400 analyses, 50 images, 9 fragments of layer-by-layer core samples) 18 mineral phases and their 12 varieties were diagnosed. The most common are iron-magnesium and calcium-bearing varieties of silicates – anortite, clinopyroxenes and olivine. The typomorphic features of rock-forming minerals in two types of the lunar surface are discussed. The composition of chromespinelids is demonstrated on a triangular prism diagram.

Key words: Moon, Soviet automatic stations, Lunar regolith, Mare Fecunditatis, sea of Crises, anorthite, clinopyroxen, olivine, ilmenite, olivine gabbro

Recommended citation: Makeyev A.B., Bryanchaninova N.I. (2021). Typomorphism of rock-forming minerals of Lunar regolith, Luna-16, -20, -24: comparision of sea vs continent vs sea. *Georesursy = Georesources*, 23(1), pp. 94–105. DOI: https://doi.org/10.18599/grs.2021.1.10

Introduction

The achievements of American and Russian scientists in the study of the mineralogy of the Moon, which are described in numerous monographs and thousands of articles (Barsukov, 1977; Bogatikov, Makeyev, 2012; Regolith from the highland region of the Moon, 1979; Lunar soil from Mare Crisium..., 1980; Khisina, 1987; Magmatism of the Earth and the Moon..., 1990; Malysheva, 1980; Mokhov, et al., 2007; Heggerty, 1979; Frondel, 1978; The Moon..., 1977; and many others) and undoubdfully outstanding. Nevertheless it often pays off to resume the studies of the old samples decades later using new approaches, modern technical and analytical capabilities. Over 100 mineral arts have been diagnosed on the lunar surface by now (Frondel, 1978, Mokhov et al., 2007). We were able to identify only a fifth of these minerals in the studied material. The purpose of this work is not to complete the list of diagnosed minerals, but to identify typomorphic features of the main rock-forming minerals on the core material of three automatic stations in the sea – continent – sea profile.

The mail goal of the study of lunar rocks and minerals of regolith sampleas from stations Luna-16, -20, -24 is the comparison of the mineral composition and changes in the chemical characteristics of rock-forming minerals of lunar rocks in the three regions from Mare Fecunditatis through the continental area to Mare Crisium. There were received over 50 electron microscopic images of the particles (Fig. 1−3) in back-scattered electron method (BSE) and the composition of mineral phases of regolith (in polished preparations), more than 400 original microprobe analyses at the electron microscope JEOL JXA-8200 with 5 wave spectrometers and scanning electron microscope JSM-5610LV with energy dispersive console‘s standard settings. We have diagnosed 18 mineral phases and their 12 variations (Table 1), the most interesting new findings are presented in Tables 2−6. The recalculation of the composition of minerals into minals and crystallochemical coefficients in Tables 2–6 was carried out by the charge method.

Let us examine the distribution of petrographic rock types on the Lunar surface in the profile alignment of Luna-16, -20, -24 stations. According to electron microscopic images of preparations of regolith grains (Fig. 1−3), namely, their mineral composition, mineral ratio, as well as structural and textural features, we diagnose there types of rocks. On the territory of the lunar seas (stations Luna-16, -24), the most common are fragments of basalt grains, olivine basalts, orange and green glasses, rocks with traces of impact and partial melting (bubble basalts, breccias, agglomerates), as well as small fragments of the main rock-forming silicates – olivine, plagioclase and clinopyroxenes. On the continental part of the Moon (Luna-20), the composition

*Corresponding author: Alexander B. Makeyev
E-mail: abmakeev@mail.ru

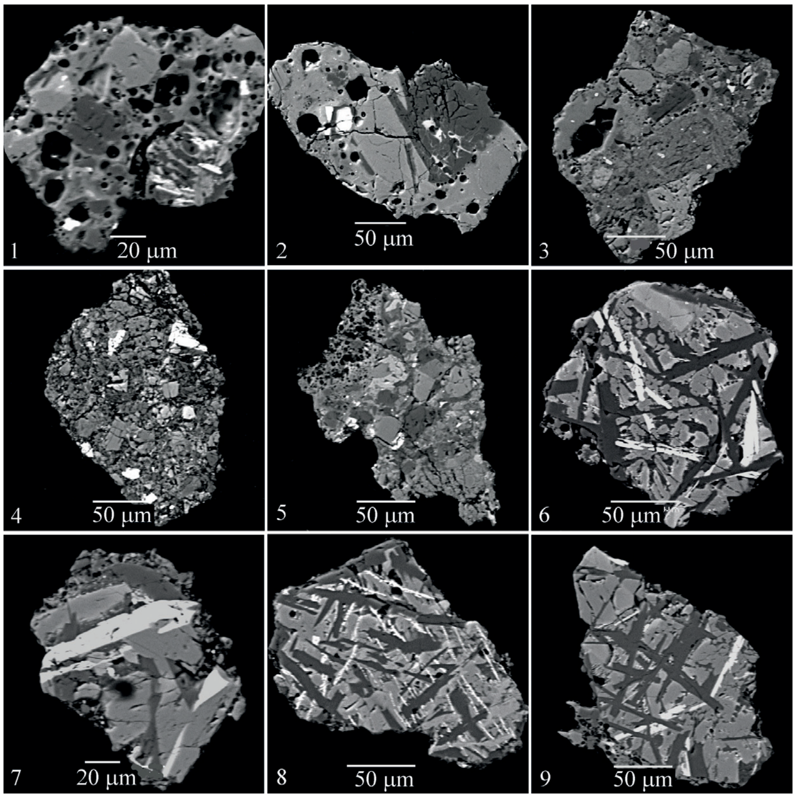

Fig. 1. Electron microscopic images (BSE) of the Luna-16 regolith grain. 1–5 – breccia of marine basalt (Cpx>Pl>Ol>Gls); 6–9 – olivine basalt (Cpx>Pl>Ol), olivine with spinifex structure. The main rock-forming minerals: olivine (white), clinopyroxene (light gray), plagioclase-anorthite (dark gray), glass (dark).

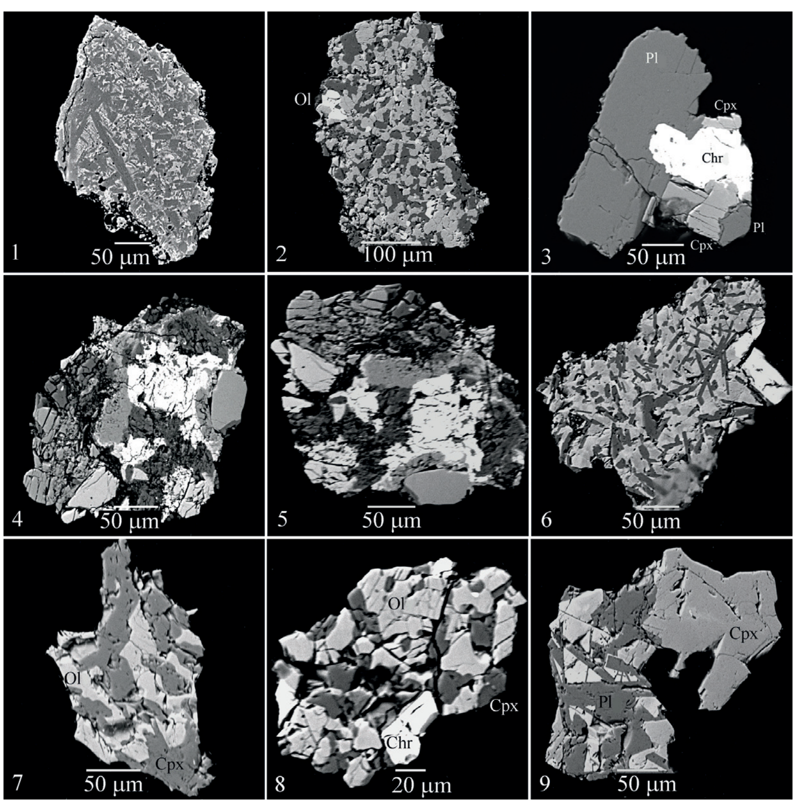

Fig. 2. Electron microscopic images (BSE) of lunar regolith grains Luna-20. 1 – aphanite gabbro; 2, 3 – gabbro with chromespinelide (alumochromite); 4, 5 – brecciated olivine gabbro (Ol>Cpx>Pl); 6 – olivine gabbro (Cpx>Pl>Ol); 7 – verlite (Cpx=Ol); 8 – brecciated verlite (Ol>Cpx>Chr); 9 – gabbro (Cpx>Pl).

of rocks is radically different: gabbro, olivine gabbro, and verlites predominate here. Other sources also report wide distribution of anorthosites with pink spinel in the continental regions, the "Mg-suite" rocks of dunites, troctolites, norites, gabbro-norites, and occurance of mantle rocks of lherzolites on the far side of the Moon (Prissel et al., 2014).

It is very likely that the collected lunar regolith grains at the point of observation of automatic stations were actually geathered on the area of several hectares. Meteorite bombardment of the surface leads to the layer-by-layer accumulation of fragments of local rocks and material mixing. Large chunks of rock may fly off further, and the fine material of the psephite and siltstone fractions remains close to the impact site. It is known form other studies, that the material delivered to the Earth by automatic stations is quite homogeneous in its chemical core composition, as analyzed by taking a variety

Rock-forming minerals	L-16	L-20	L-24	Σ
Anortite	13	17	16	46
Bitovnite	9			9
Forsterite		2	1	3
Gortonolite 0.20-0.80 (Fa)	13	11	16	40
Faylite		2	4	6
Augite	13	5	21	39
Ferroaugite	5	7	22	34
Subcalcic augite	3	5	11	19
Subcalcic ferroaugite	8	10	22	40
Magnesia pigeonite	2		4	6
Intermediate pigeonite	3	4	7	14
Ferrous pigeonite		1	1	2
Hedenbergite	3	2	10	15
Ferrosalite	2			2
Pyroxferroite	4			4
Clinoenstatite			1	1
Orthopyroxene - *bronzite*		3		3
Sum:	78	69	136	283
Accessory minerals	L-16	L-20	L-24	Σ
Chromite, chromespinelides				
Subalumotitanochromite		3	9	12
Subalumosubtitanochromite		1	2	3
Ulvoshpinel		2	6	8
Chrom-ulvoshpinel	5	8	2	15
Ilmenite	21	1	10	32
Native iron, Kamasite	1	1	1	3
Tenite ($Fe_{0,75}Ni_{0,25}$)	1		1	2
Troilite	1	2	14	17
Pyrrhotite	4			4
Tranquilitiite	1			1
Vitlokite	1			1
Quartz (SiO_2)		1	1	2
Basalt glass	3	3	3	9
Glass (garnet type)	9			9
Sum:	47	22	49	118

Table 1. Occurrence of mineral phases and their varieties (number of analyses) in the lunar regolith at the landing sites of Luna-16, -20, -24 stations. Mineral varieties are shown in italics.

of small samples from different core depths (Barsukov, 1977; Bell et al., 1978; Taylor et al., 1978; etc.). To determine the average mineral composition of primary rocks (for example, Luna-24 regolith), we conducted a standard mineral recalculation of 40 complete chemical analyses performed on the core column material in bound layer-by-layer samples from several published works, and in GEOHI named after V.I. Vernadsky's analyses were carried out by the wet chemical method, as well as in foreign scientific centers – by the X-ray fluorescence method. For the recalculations we used the average compositions of rock-forming minerals (Tables 2–4). The standard conversion method used: 1. The content of plagioclase is calculated from the amount of Na_2O in the sample; 2. The amount of CaO in already defined plagioclase is calculated; 3. The calculated calcium in the plagioclase is being subtracted from the total amount of CaO; 4. The standard content of clinopyroxene is calculated from the CaO residue (using its average composition from Table 2); 5. The content of basalt glass in rocks is assumed to be 4 vol.%, its composition is known from the existing study (Bell et al., 1978), it is close to the composition of clinopyroxene; 6. The content of olivine is calculated as the remainder of the three previously defined components (Ol = 100-Pl-Cpx-Gls). Finally, the presence of three primary rocks in the core of Luna-24 was determined: non-olivine basalt (n=24 Pl – 36, Cpx – 60, Gls – 4 vol.%); olivine basalt (n=11 Pl – 40, Cpx – 42, Ol – 14, Gls – 4 vol.%); picrobasalt and picrite (n=5 Pl – 25, Cpx – 29, Ol – 42, Gls – 4 vol.%).

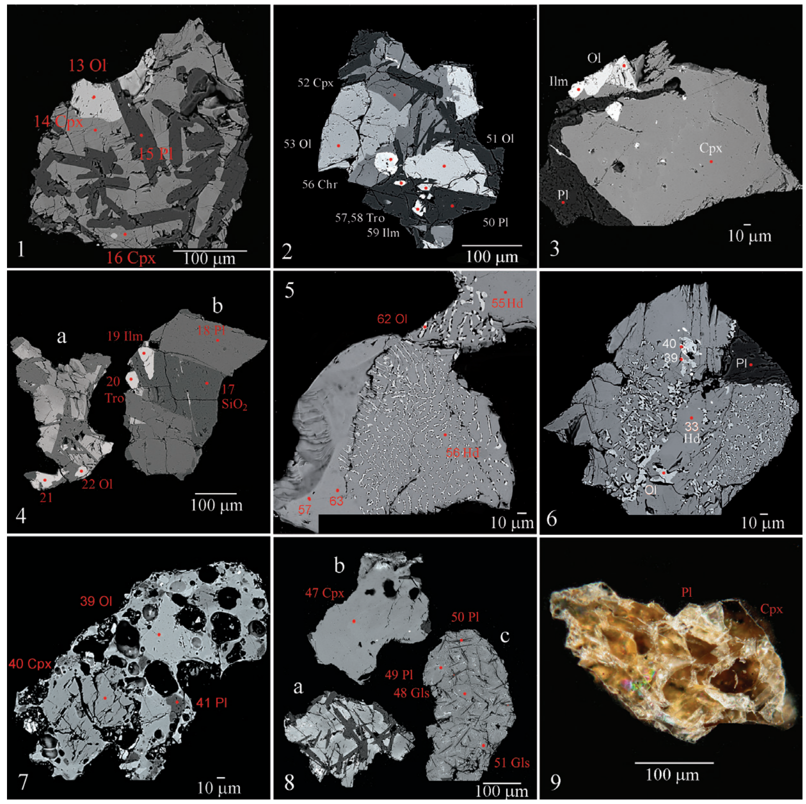

Fig. 3. Electron microscopic (1-8), BSE mode, and optical (9) images of Luna-24 regolith grains. 1–3. 4(a) – olivine basalt with ilmenite and troilite; 4 (b) – "quartz" veins in plagioclase with ilmenite and troilite; 5, 6 – structures of liquid immiscibility of olivine-pyroxene melt; 7 – bubble basalt; 8 – (a) basalt (Cpx>Plg), (b) clinopyroxene, (c) basalt glass; 9 – basalt (Cpx>Plg), petrographic microscope dark field image, pyroxene (brown), anorthite (white). The points of microprobe analyses are marked. Symbols: Cpx – clinopyroxene; Chr – subtitanoalumochromite; Hd – hedenbergite; Gls – glass; Ilm – ilmenite; Ol – olivine (gortonolite and fayalite); Pl – anorthite; Tro – troilite

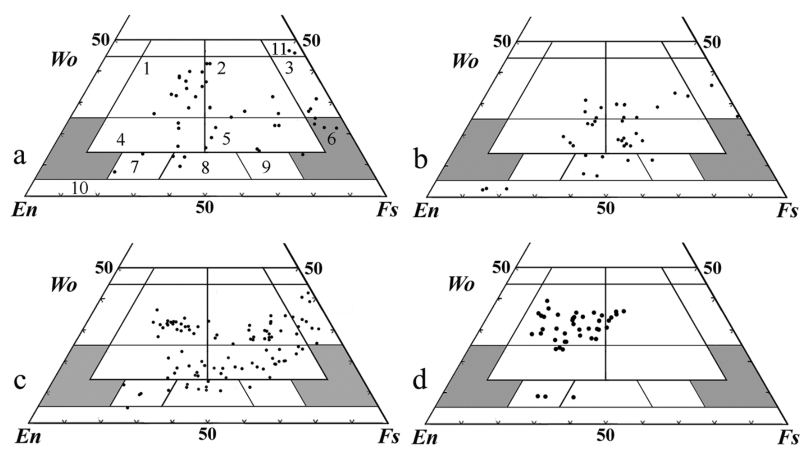

Fig. 4. Diagram of the composition of Lunar regolith pyroxenes: a – Luna-16, b – Luna-20, c – Luna-24 stations, and terrestrial tholeitic basalts (d) (Makeyev, Bryanchaninova, 2007). 1 – augite, 2 – ferroaugite, 3 – hedenbergite, 4 – subcalcic augite, 5 – subcalcic ferroaugite, 6 – pyroxferroite, 7 – magnesia pigeonite, 8 – intermediate pigeonite, 9 – ferrous pigeonite, 10 – clinoenstatite, 11 – ferrocalite

Results

All the studied regolith particles are fragments of lunar rocks with a size of 100–500 µm have a retained micrograin structure with a set of minerals characteristic of olivine basalts, gabbro, verlites, slag-like particles, breccias and other rocks (Fig. 1–3). The grains of rocks and minerals are fractured, the fragments of rocks have a cancellous fracture, the grains of minerals that have cleavage are split by cleavage. We have not encountered any fragments of meteorite material. In addition to the grains of debris, there are fragments of large particles (50–450 µm) of the same lunar minerals from basalts and other rocks – anorthite, olivine, pyroxenes, which have a predominant distribution. Ore minerals: native metals, oxides, and sulfides with a size of 1–50 µm are found only as inclusions in other silicate minerals. It is

L-16

Oxides	1	2	3	4	5	6	7	8	9	10	11	12	13	14	15	16	17	18	19	20	21	22	23	Aver.
SiO_2	47.87	48.40	49.00	49.23	46.43	50.46	50.40	50.05	50.84	53.09	54.32	51.37	50.60	51.16	48.16	49.60	48.19	46.51	45.93	45.58	45.81	46.20	46.29	48.93
TiO_2	2.64	2.43	1.77	2.20	3.40	1.95	1.09	1.77	0.61	0.07	0.28	0.58	0.52	0.56	1.01	0.99	1.00	1.98	1.53	1.52	1.03	1.25	0.69	1.34
Al_2O_3	3.46	3.63	1.96	2.19	4.45	2.05	1.87	1.91	1.57	1.30	1.10	1.03	1.61	1.51	1.21	1.10	1.33	1.80	1.10	1.49	1.81	1.04	1.16	1.81
Cr_2O_3	0.48	0.41	0.38	0.35	0.30	0.77	0.52	0.05	0.53	0.51	0.59	0.21	0.42	0.51	0.00	0.28	0.28	0.09	0.17	0.00	0.00	0.07	0.18	0.31
FeO	15.99	14.54	18.94	15.87	16.70	13.69	18.79	18.86	21.72	16.22	13.68	23.95	23.53	21.53	32.58	26.11	28.68	28.95	36.98	35.80	37.99	37.54	39.22	24.25
MnO	0.24	0.35	0.22	0.30	0.16	0.17	0.33	0.41	0.44	0.45	0.13	0.03	0.33	0.47	0.68	0.40	0.36	0.73	0.73	0.73	0.59	0.37	0.47	0.40
MgO	12.05	14.84	12.21	13.91	12.21	18.02	15.90	16.14	16.47	21.23	26.19	18.08	16.39	17.59	9.25	12.66	7.73	5.20	2.54	1.31	2.65	2.58	2.27	12.06
CaO	17.28	15.40	15.52	15.95	16.35	12.89	11.10	10.80	7.82	7.11	3.71	4.75	6.60	6.67	7.11	8.85	12.42	14.74	11.02	13.57	10.13	10.95	9.73	10.89
Sum	100.0	100.0	100.0	100.0	100.0	100.0	100.0	100.0	100.0	100.0	100.0	100.0	100.0	100.0	100.0	100.0	100.0	100.0	100.0	100.0	100.0	100.0	100.0	100.0
Si^{4+}	0.937	0.934	0.956	0.950	0.915	0.955	0.968	0.960	0.979	0.989	0.988	0.982	0.977	0.980	0.974	0.976	0.974	0.954	0.968	0.963	0.967	0.972	0.979	0.965
Ti^{4+}	0.039	0.035	0.026	0.032	0.050	0.028	0.016	0.026	0.009	0.001	0.004	0.008	0.008	0.008	0.015	0.015	0.015	0.031	0.024	0.024	0.016	0.020	0.011	0.020
Al^{IV}	0.024	0.030	0.018	0.018	0.035	0.017	0.016	0.015	0.013	0.010	0.008	0.009	0.015	0.012	0.010	0.009	0.011	0.015	0.008	0.013	0.016	0.008	0.010	0.015
Al^{VI}	0.016	0.011	0.005	0.007	0.017	0.005	0.005	0.007	0.005	0.005	0.003	0.002	0.003	0.005	0.004	0.003	0.005	0.007	0.006	0.006	0.006	0.005	0.005	0.006
Cr^{3+}	0.004	0.003	0.003	0.003	0.002	0.006	0.004	0.000	0.004	0.004	0.004	0.002	0.003	0.004	0.000	0.002	0.002	0.001	0.001	0.000	0.000	0.001	0.001	0.002
Fe^{2+}	0.262	0.235	0.309	0.256	0.275	0.217	0.302	0.302	0.350	0.253	0.208	0.383	0.380	0.345	0.551	0.430	0.485	0.497	0.652	0.632	0.671	0.660	0.694	0.406
Mn^{2+}	0.004	0.006	0.004	0.005	0.003	0.003	0.005	0.007	0.007	0.007	0.002	0.000	0.005	0.008	0.012	0.007	0.006	0.013	0.013	0.013	0.010	0.007	0.008	0.007
Mg^{2+}	0.352	0.427	0.355	0.400	0.359	0.508	0.455	0.462	0.473	0.590	0.710	0.515	0.472	0.502	0.279	0.371	0.233	0.159	0.080	0.041	0.083	0.081	0.072	0.347
Ca^{2+}	0.363	0.318	0.325	0.330	0.345	0.261	0.228	0.222	0.161	0.142	0.072	0.097	0.136	0.137	0.154	0.187	0.269	0.324	0.249	0.307	0.229	0.247	0.220	0.231
Ca/Ca+Mg	0.507	0.427	0.477	0.452	0.490	0.339	0.334	0.325	0.254	0.194	0.092	0.159	0.224	0.214	0.356	0.334	0.536	0.671	0.757	0.882	0.733	0.753	0.755	0.446
Fs	26.82	23.94	31.25	25.96	28.10	21.96	30.63	30.68	35.55	25.68	21.00	38.46	38.44	35.05	55.99	43.50	49.13	50.70	66.48	64.47	68.22	66.84	70.38	41.27
En	36.05	43.57	35.92	40.59	36.64	51.55	46.20	46.81	48.06	59.90	71.70	51.77	47.75	51.04	28.35	37.61	23.60	16.24	8.14	4.20	8.48	8.18	7.26	35.20
Wo	37.14	32.49	32.82	33.44	35.25	26.49	23.17	22.51	16.39	14.42	7.30	9.77	13.81	13.91	15.65	18.90	27.27	33.07	25.38	31.32	23.30	24.98	22.36	23.53
Type. Subtype	Augite						*Subcalcium augite*			*Magnesia pigeonite*		*Intermediate pigeonite*			*Subcalcic ferroaugite*		*Ferroaugite*		*Hedenbergite*		Pyroxferroite			

Table 2. Chemical composition of pyroxenes (wt.%) of the lunar regolith, formula coefficients and minals Luna-16 Station, Luna-20 Station, Luna-24 Station. Pyroxene analyses were performed on the JEOL JXA-8200 device, analyst – A.A. Virus.

very important to note the color of the three most common silicate minerals observed under binoculars and in a petrographic microscope in the „dark field": anorthite – gray, dark gray; olivine – dark green, brown; clinopyroxene – brown (Fig. 3 *9*), dark brown (due to high glandular content). Due to that fact the characteristic brown color of the regolith of the lunar surface in modern color cosmic images is observed.

Less common are baked microbreccia of rocks and the same minerals (Fig. 1 *3–5*; Fig. 2 *4,5*), basalts with characteristic (Fig. 1 *6,7*) spinifex-form selections of olivine, rounded fragments of basaltic glass (Fig. 3 *8s*) with detected microcrystals of anortite and olivine; the composition of the two particles of hedenbergite (Fig. 3 *5,6*) with lamellies of olivine-fayalite and inclusions of ilmenite and troilite was discovered as well. The micrograin structure of marine basalt fragments in the lunar regolith indicates a very rapid crystallization of basalts.

Analysis of images (structures and textures) of rocks allows us to establish sequence of mineral extraction in the lunar olivine basalt: 1) olivine and chromian spinel are → 2) clinopyroxene → 3) plagioclase (anortite) → 4) ilmenite, ulvospinel, sulfides (of troilite, etc.).

A comparison of the mineral composition and textures of non-metamorphosed terrestrial tholeiitic basalts with lunar marine and continental rocks revealed a significant difference in the appearance and set of rocks, the composition of mineral phases. The isomorphic series and mineral series are dominated by calcium and ferruginous varieties. So among pyroxenes (*ferroaugite, subcalcic ferroaugite, hedenbergite, intermediate pianet*), and among the olivine – *hortonolite* and fayalite (Tables 2, 3; Fig. 4, 5) i.e. their glandular species, and among the high calcium plagioclase anortite.

Clinopyroxenes

Pyroxenes from terrestrial basalts are always of variable composition, usually zonal with a change in composition from the grain center to the periphery, so *subcalcium augite* is replaced by augite and *ferroaugite* (Makeyev and Bryanchaninova, 2007), from calcium-magnesium to ferruginous varieties of clinopyroxenes (Fig. 4d). In lunar basalts, zoning is not so pronounced, however,

L-20

Oxides	1	2	3	4	5	6	7	8	9	10	11	12	13	14	15	16	17	18	19	20	21	22	23	Aver.
SiO_2	45.86	49.97	49.52	49.39	48.81	50.14	49.33	47.35	48.60	54.88	50.26	51.76	51.34	50.60	46.38	50.10	49.77	48.69	48.24	48.52	49.26	47.62	41.18	49.02
TiO_2	0.76	0.35	0.55	0.47	0.82	0.33	0.56	0.53	0.63	0.00	0.52	0.39	0.12	0.48	0.07	0.06	0.33	1.37	0.53	0.92	1.06	1.12	3.90	0.69
Al_2O_3	10.47	2.35	1.24	1.38	2.01	0.59	1.12	3.82	1.85	1.09	2.05	1.07	3.00	1.50	9.08	2.67	1.10	1.27	1.64	1.55	1.45	0.81	4.47	2.50
Cr_2O_3	0.77	0.39	0.41	0.10	0.15	0.22	0.17	0.38	0.33	0.77	0.79	0.53	0.34	0.46	0.06	0.22	0.00	0.43	0.16	0.50	0.26	0.15	0.16	0.34
FeO	16.69	20.81	25.88	28.19	27.86	28.16	28.89	29.54	28.42	13.86	20.29	19.58	17.55	21.45	23.57	27.48	30.00	24.76	28.87	27.14	23.11	30.40	39.43	25.30
MnO	0.13	0.25	0.34	0.30	0.35	0.44	0.76	0.40	0.31	0.15	0.26	0.51	0.25	0.37	0.33	0.36	0.50	0.18	0.41	0.48	0.53	0.36	0.39	0.36
MgO	13.46	12.27	10.80	10.99	11.26	11.82	11.18	9.61	9.85	27.97	14.49	17.45	17.97	14.34	17.38	16.00	12.07	9.58	6.93	9.26	10.61	4.62	0.00	12.17
CaO	11.87	13.61	11.25	9.17	8.75	8.30	7.99	8.36	10.00	1.29	11.33	8.71	9.43	10.80	3.14	3.11	6.22	13.72	13.22	11.62	13.72	14.92	10.48	9.61
Sum	100.0	100.0	100.0	100.0	100.0	100.0	100.0	100.0	100.0	100.0	100.0	100.0	100.0	100.0	100.0	100.0	100.0	100.0	100.0	100.0	100.0	100.0	100.0	100.0
Si^{4+}	0.920	0.977	0.981	0.981	0.972	0.990	0.982	0.962	0.975	0.992	0.975	0.985	0.977	0.980	0.918	0.980	0.987	0.969	0.978	0.973	0.973	0.976	0.902	0.970
Ti^{4+}	0.011	0.005	0.008	0.007	0.012	0.005	0.008	0.008	0.010	0.000	0.008	0.006	0.002	0.007	0.001	0.001	0.005	0.021	0.008	0.014	0.016	0.017	0.064	0.011
Al^{IV}	0.069	0.017	0.010	0.011	0.016	0.005	0.010	0.030	0.016	0.008	0.017	0.009	0.022	0.013	0.081	0.019	0.008	0.010	0.014	0.013	0.012	0.007	0.034	0.020
Al^{VI}	0.055	0.010	0.004	0.005	0.008	0.002	0.003	0.015	0.006	0.004	0.006	0.003	0.012	0.005	0.025	0.011	0.005	0.005	0.006	0.006	0.005	0.003	0.024	0.010
Cr^{3+}	0.006	0.003	0.003	0.000	0.001	0.002	0.001	0.003	0.003	0.006	0.006	0.004	0.003	0.004	0.000	0.002	0.000	0.003	0.001	0.004	0.002	0.001	0.001	0.003
Fe^{2+}	0.280	0.340	0.429	0.468	0.464	0.465	0.481	0.502	0.477	0.209	0.329	0.312	0.279	0.347	0.390	0.449	0.498	0.412	0.489	0.455	0.382	0.521	0.722	0.422
Mn^{2+}	0.002	0.004	0.006	0.005	0.006	0.007	0.013	0.007	0.005	0.002	0.004	0.008	0.004	0.006	0.006	0.006	0.008	0.003	0.007	0.008	0.009	0.006	0.007	0.006
Mg^{2+}	0.402	0.358	0.319	0.326	0.334	0.348	0.332	0.291	0.295	0.754	0.419	0.495	0.510	0.414	0.513	0.467	0.357	0.284	0.209	0.277	0.312	0.141	0.000	0.355
Ca^{2+}	0.255	0.285	0.239	0.195	0.187	0.176	0.170	0.182	0.215	0.025	0.236	0.178	0.192	0.224	0.066	0.065	0.132	0.293	0.287	0.250	0.290	0.328	0.246	0.205
Ca/Ca+Mg	0.388	0.444	0.428	0.375	0.358	0.335	0.339	0.385	0.422	0.032	0.360	0.264	0.274	0.351	0.115	0.123	0.270	0.507	0.578	0.474	0.482	0.699	1.000	0.391
Fs	29.86	34.60	43.46	47.34	47.11	47.04	48.92	51.48	48.33	21.20	33.46	31.66	28.46	35.24	40.24	45.80	50.42	41.68	49.64	46.36	38.78	52.64	74.60	42.97
En	42.92	36.39	32.34	32.92	33.95	35.20	33.75	29.85	29.87	76.28	42.59	50.29	51.94	42.02	52.90	47.56	36.17	28.73	21.24	28.21	31.73	14.25	0.00	36.14
Wo	27.22	29.01	24.20	19.74	18.95	17.76	17.34	18.67	21.80	2.52	23.95	18.05	19.60	22.73	6.86	6.65	13.40	29.59	29.11	25.43	29.50	33.11	25.40	20.89
Type. *Subtype*	Augite		*Subcalcic ferroaugite*						*Magnesia pigeonite*						*Intermediate pigeonite*			*Ferroaugite*				*Hedenbergite*		

Table 2. Continuation

in single small regolith particles of 300–500 μm, as a rule, several phases of pyroxenes of different composition are found, and structures of liquid immiscibility of olivine-pyroxene melt (Fig. 3 *5,6*) are often observed (Khisina, 1987).

This observation is interpreted by us as a significant difference in the longevity of crystallization of basaltic magma: on Earth, it took long for magma to cool down, allowing the crystallization of minerals with a change in their chemistry in individual grains, on the Moon, to the contrary, a very fast crystallization led to a fixed composition of mineral phases (Khisina, Makarov, 1977). Lunar basalt pyroxenes differ from the terrestrial ones significantly: they are more ferruginous and demonstrate a higher variety of their types. The lunar regolith contains three mineral types of clinopyroxene – augite, pigeonite, and clinoenstatite, as well as the pyroxenoid pyroxferroite and one type of orthopyroxene – *bronzite*, as well as 8 chemical varieties of pyroxenes (Table 2, Fig. 4): *ferroaugite, subcalcic augite, subcalcic ferroaugite, magnesia pigeonite, intermediate pigeonite*, *ferrous pigeonite*, *hedenbergite*, *ferrosalite* and terrestrial rocks (Bogatikov, 1979; Krivolutskaya, Bryanchaninova, 2011; Magmatism..., 1990; Makeyev, Bryanchaninova, 1999; 2007; Makeyev et al., 2020) distributed by the same minerals augite and pigeonite, but considerably less varieties – *ferroaugite, subcalcic augite, magnesia pigeonite*, *intermediate pigeonite*. Chromium (0.05–0.87 wt.% Cr_2O_3) and titanium (0.06–1.37 wt.% TiO_2) is a significant isomorphic impurity in lunar pyroxenes, these are potential resources from which ore ilmenite and chromite accumulations can form during recrystallization, just as it occurs in terrestrial alpine-type ultrabasites (Makeyev, Bryanchaninova, 1999).

Olivine

In lunar rocks olivine basalts, gabbro and verlite olivine are one of the main rock-forming minerals. Its peculiarity is an abnormally high glandular content. It is represented by *gortonolite* and

L-24

Oxides	1	2	3	4	5	6	7	8	9	10	11	12	13	14	15	16	17	18	19	20	21	22	23	Aver.
SiO_2	51.14	50.89	49.99	51.20	51.55	51.07	48.22	49.91	50.70	49.57	48.35	48.23	48.05	49.31	49.31	48.75	48.60	47.35	47.17	46.86	47.30	47.18	53.51	49.31
TiO_2	0.68	0.77	1.02	0.45	0.51	0.72	0.32	0.53	0.65	1.05	0.80	0.89	0.83	1.19	0.86	0.80	0.69	0.75	0.98	0.78	0.92	0.90	0.67	0.77
Al_2O_3	1.56	1.64	1.58	1.98	1.80	1.82	1.95	2.27	1.44	1.26	0.81	0.97	1.09	2.76	0.98	1.00	1.06	0.83	0.94	0.86	1.29	0.79	0.82	1.37
Cr_2O_3	0.59	0.45	0.43	0.86	0.87	0.71	0.50	0.73	0.57	0.20	0.00	0.11	0.18	0.59	0.16	0.21	0.18	0.10	0.00	0.00	0.00	0.00	0.26	0.33
FeO	14.7	15.5	17.8	12.3	14.6	14.0	13.4	18.5	16.2	24.8	29.9	28.5	29.3	22.1	27.7	29.9	27.9	33.8	31.1	37.9	32.6	33.7	16.7	23.61
MnO	0.22	0.21	0.21	0.20	0.18	0.22	0.19	0.27	0.24	0.25	0.29	0.26	0.33	0.28	0.22	0.33	0.24	0.39	0.19	0.36	0.26	0.27	0.24	0.25
MgO	14.0	13.2	11.4	15.2	16.3	15.3	13.1	13.2	14.0	10.8	6.5	5.5	6.6	11.9	7.7	6.2	7.9	3.7	1.1	2.2	2.5	2.3	25.0	9.81
CaO	16.2	16.1	16.3	16.3	13.5	15.5	14.8	14.0	15.6	11.7	13.3	15.5	13.6	12.7	12.3	12.7	11.9	13.0	18.3	11.0	15.2	14.9	2.3	13.77
Sum	99.13	98.81	98.71	98.53	99.32	99.27	92.51	99.42	99.31	99.61	100.0	100.0	100.0	100.8	99.17	99.93	98.57	99.97	99.76	99.92	99.94	100.00	99.52	99.23
Si^{4+}	0.988	0.991	0.986	0.988	0.987	0.980	0.999	0.975	0.980	0.984	0.980	0.980	0.974	0.965	1.001	0.993	0.992	0.981	0.984	0.987	0.984	0.982	0.986	0.985
Ti^{4+}	0.010	0.011	0.015	0.006	0.007	0.010	0.005	0.008	0.009	0.016	0.012	0.014	0.013	0.018	0.013	0.012	0.011	0.012	0.015	0.012	0.014	0.014	0.009	0.012
Al^{IV}	0.003	0.000	0.000	0.006	0.005	0.009	0.000	0.017	0.011	0.000	0.008	0.006	0.013	0.017	0.000	0.000	0.000	0.008	0.001	0.001	0.001	0.004	0.005	0.005
Al^{VI}	0.015	0.021	0.020	0.017	0.015	0.011	0.027	0.009	0.006	0.014	0.002	0.005	0.000	0.015	0.026	0.017	0.015	0.003	0.011	0.010	0.015	0.006	0.004	0.012
Cr^{3+}	0.004	0.003	0.003	0.007	0.007	0.005	0.004	0.006	0.004	0.002	0.000	0.001	0.001	0.005	0.001	0.002	0.001	0.001	0.000	0.000	0.000	0.000	0.002	0.003
Fe^{2+}	0.238	0.253	0.294	0.199	0.235	0.224	0.232	0.302	0.261	0.412	0.507	0.484	0.497	0.362	0.469	0.510	0.477	0.585	0.542	0.667	0.567	0.587	0.258	0.398
Mn^{2+}	0.004	0.004	0.003	0.003	0.003	0.003	0.003	0.004	0.004	0.004	0.005	0.004	0.006	0.005	0.004	0.006	0.004	0.007	0.003	0.006	0.005	0.005	0.004	0.004
Mg^{2+}	0.404	0.384	0.334	0.438	0.464	0.437	0.404	0.385	0.402	0.320	0.197	0.168	0.200	0.347	0.233	0.188	0.242	0.116	0.035	0.069	0.076	0.072	0.688	0.287
Ca^{2+}	0.335	0.335	0.345	0.337	0.277	0.319	0.329	0.293	0.323	0.248	0.289	0.338	0.295	0.267	0.268	0.277	0.261	0.289	0.408	0.248	0.338	0.331	0.045	0.295
Ca/Ca+Mg	0.453	0.466	0.508	0.435	0.374	0.422	0.449	0.432	0.445	0.437	0.595	0.668	0.596	0.435	0.535	0.595	0.519	0.714	0.920	0.784	0.816	0.822	0.061	0.543
Fs	24.4	26.0	30.2	20.4	24.0	22.9	24.1	30.8	26.5	42.0	51.1	48.9	50.0	37.1	48.4	52.3	48.7	59.1	55.0	67.8	57.8	59.3	26.0	40.6
En	41.4	39.5	34.3	45.0	47.6	44.6	41.8	39.3	40.8	32.7	19.8	17.0	20.2	35.6	24.0	19.3	24.7	11.7	3.6	7.0	7.8	7.2	69.5	29.3
Wo	34.3	34.5	35.5	34.6	28.4	32.5	34.1	29.9	32.7	25.3	29.1	34.1	29.8	27.4	27.6	28.4	26.7	29.2	41.4	25.2	34.4	33.5	4.5	30.1
Type. *Subtype*	Augite									*Ferroaugite*									*Hedenbergite*				Clino-enstatite	

Table 2. Continuation

fayalite (Table 3, Fig. 5). Among the isomorphic impurities in olivines, manganese is common, the same pattern we observe in lunar ones (0.10–0.95 wt.% MnO); nickel in lunar olivines was hardly detectable, whereas the calcium content is much higher (0.08–2.87 wt.% CaO), and in marine basalts even more than in continental areas and even higher than in terrestrial ones (Makeyev, Bryanchaninova, 1999). In the book "Magmatism of the Earth and the Moon" (1990), dwells on the isomorphic occurrence of chromium in the lunar olivines, established in the amount of (0.03–0.32 wt.% Cr_2O_3). In the terrestrial olivines of ultrabasites and basites, chromium is absent, although there are rare references to exceptions in the literature (Magmatism of the Earth and the Moon..., 1990).

Plagioclase

Lunar pyroxenes in marine basalts and gabbro are associated with high-calcium plagioclase anorthite – $An_{0,90\text{-}1,00}$ or very rarely with bitovnite – $An_{0,80\text{-}0,90}$ (Table 4, Fig. 6). Anorthite prevails. In terrestrial basalts we often observe basic plagioclase labradorite-bytownite, and very rarely – andesine. The peculiarity of lunar plagioclases is the low sodium content (0.07–3.12 wt.% Na_2O), and an abnormally high iron content (0.01–2.26 wt.% FeO), which can only be explained by invisible inclusions of other ferrous minerals. In cases when the size of the rock fragments achieves 100–500 μm, the dimensions of rather perfect plate-like plagioclase crystals are often up to 3–50 μm in width, and 10–300 μm in length.

The main accessory ore minerals of terrestrial basalts and basic igneous rocks (specialized for titanium-iron ores) are titanomagnetite, ilmenite, pyrite and chalcopyrite, and in lunar ones – ilmenite, ulvoshpinel, subalumotitanochromite, troilite, pyrrhotite and native iron.

Ilmenite

Small inclusions of ilmenite are widely distributed in the basalts of the lunar seas (Luna-16, -24). The chemical composition of the studied grains is

L-24

Oxides	24	25	26	27	28	29	30	31	32	33	34	35	36	37	38	39	40	41	42	43	44	45	46	Aver.
SiO_2	50.15	50.53	51.40	50.63	51.52	51.35	49.95	49.20	48.35	48.54	47.49	47.59	48.10	47.56	49.95	49.30	50.98	49.51	49.80	51.78	53.11	53.11	52.99	50.12
TiO_2	0.36	0.31	0.26	0.30	0.27	0.32	0.43	0.76	0.60	0.59	0.87	0.73	0.86	0.83	0.40	0.41	0.51	0.87	0.78	0.53	0.12	0.32	0.12	0.50
Al_2O_3	1.68	1.12	1.40	1.27	1.86	1.28	1.19	0.82	0.83	0.93	1.00	0.79	0.82	0.78	0.91	0.61	0.97	1.21	0.91	1.10	1.10	1.20	1.27	1.09
Cr_2O_3	0.75	0.50	0.59	0.55	0.83	0.52	0.39	0.12	0.15	0.14	0.00	0.00	0.16	0.00	0.24	0.20	0.29	0.22	0.23	0.51	0.66	0.74	0.63	0.37
FeO	20.39	24.63	20.24	24.93	17.69	22.41	26.48	30.52	34.38	31.03	36.00	35.83	32.36	35.54	27.83	32.80	23.99	29.92	27.47	21.07	17.27	12.72	17.34	26.21
MnO	0.25	0.29	0.30	0.30	0.24	0.32	0.31	0.37	0.40	0.44	0.33	0.36	0.38	0.39	0.34	0.35	0.34	0.33	0.34	0.28	0.24	0.16	0.21	0.32
MgO	14.78	14.56	17.28	14.38	16.81	15.34	12.19	9.04	7.00	7.01	4.08	4.74	7.12	4.07	11.64	10.59	16.12	12.51	13.47	19.13	22.59	23.75	22.52	13.07
CaO	10.85	8.05	8.54	7.51	10.28	8.77	8.30	8.44	8.55	10.62	10.68	9.88	9.75	10.84	8.45	5.58	6.31	5.26	7.00	5.35	4.49	6.54	4.94	8.04
Sum	99.22	100.0	100.0	99.88	99.49	100.3	99.23	99.27	100.3	99.30	100.5	99.92	99.54	100.0	99.76	99.83	99.51	99.81	100.0	99.75	99.58	98.53	100.0	99.72
Si^{4+}	0.977	0.983	0.982	0.989	0.989	0.989	0.993	0.997	0.986	0.993	0.983	0.986	0.984	0.987	0.991	0.991	0.988	0.985	0.978	0.985	0.990	0.988	0.985	0.987
Ti^{4+}	0.005	0.004	0.004	0.004	0.004	0.005	0.006	0.012	0.009	0.009	0.014	0.011	0.013	0.013	0.006	0.006	0.007	0.013	0.012	0.008	0.002	0.004	0.002	0.008
Al^{IV}	0.017	0.012	0.015	0.007	0.007	0.006	0.001	0.000	0.004	0.000	0.004	0.003	0.003	0.000	0.003	0.003	0.004	0.002	0.011	0.007	0.008	0.008	0.013	0.006
Al^{VI}	0.002	0.000	0.001	0.008	0.014	0.008	0.013	0.019	0.006	0.014	0.008	0.007	0.007	0.010	0.007	0.004	0.007	0.012	0.000	0.005	0.004	0.005	0.000	0.007
Cr^{3+}	0.006	0.004	0.004	0.004	0.006	0.004	0.003	0.001	0.001	0.001	0.000	0.000	0.001	0.000	0.002	0.002	0.002	0.002	0.002	0.004	0.005	0.005	0.005	0.003
Fe^{2+}	0.332	0.401	0.323	0.407	0.284	0.361	0.440	0.517	0.586	0.531	0.623	0.621	0.554	0.617	0.461	0.551	0.389	0.498	0.451	0.335	0.269	0.198	0.269	0.436
Mn^{2+}	0.004	0.005	0.005	0.005	0.004	0.005	0.005	0.006	0.007	0.008	0.006	0.006	0.007	0.007	0.006	0.006	0.006	0.006	0.006	0.004	0.004	0.002	0.003	0.005
Mg^{2+}	0.429	0.422	0.492	0.419	0.481	0.440	0.361	0.273	0.213	0.214	0.126	0.146	0.217	0.126	0.344	0.317	0.466	0.371	0.394	0.543	0.628	0.658	0.624	0.379
Ca^{2+}	0.226	0.168	0.175	0.157	0.211	0.181	0.177	0.183	0.187	0.233	0.237	0.219	0.214	0.241	0.180	0.120	0.131	0.112	0.147	0.109	0.090	0.130	0.098	0.171
Ca/Ca+Mg	0.345	0.284	0.262	0.273	0.305	0.291	0.329	0.402	0.467	0.521	0.653	0.600	0.496	0.657	0.343	0.275	0.220	0.232	0.272	0.167	0.125	0.165	0.136	0.340
Fs	33.6	40.4	32.7	41.4	29.1	36.7	45.0	53.1	59.5	54.3	63.2	62.9	56.2	62.7	46.8	55.8	39.5	50.7	45.4	34.0	27.3	20.1	27.2	44.2
En	43.5	42.6	49.7	42.6	49.3	44.8	36.9	28.0	21.6	21.9	12.8	14.8	22.1	12.8	34.9	32.1	47.3	37.8	39.7	55.0	63.6	66.7	62.9	38.4
Wo	22.9	16.9	17.6	16.0	21.6	18.4	18.1	18.8	18.9	23.8	24.0	22.2	21.7	24.5	18.2	12.2	13.3	11.4	14.8	11.1	9.1	13.2	9.9	17.3
Type. *Subtype*	*Subcalcic augite*						*Subcalcic ferroaugite*									*Intermediate pigeonite*				*Magnesia pigeonite*				

Table 2. Continuation

presented in Table 5. The average compositions of ilmenite from the regolith of the two stations are quite close to and do not differ significantly from those of the Earth, even the usual isomorphic impurities are observed: Mn, V, Cr. In the ilmenites of the Luna-24 station regolith sample, a small admixture of magnesium is present noticeably more often. In case when large accumulations of ilmenite ores are found on the Moon, they can be successfully used on an industrial scale for the production of metallic iron and rutile slag according to the well-known melt method.

Chromespinelides

Among the chromespinelides (Table 6, Fig. 7) the lunar regolith is dominated by high-iron and high-titanic *subtitanoalumochromites*. These varieties are found on Earth in ancient Archean and Proterozoic stratified ultrabasite massifs specialized for chromium ores and platinoides. The sizes of chromespinellides precipitates vary from 2–10 µm (pink spinel) to 20–130 µm – *subtitanoalumochromite* (Fig. 2 *3,8*; Fig. 3 *2*). A particular feature of lunar minerals is the absence of an oxide (trivalent) form of iron, which is proven by Mossbauer spectroscopy (Malysheva, 1980; Makeyev, 2006; 2013).

Researchers of lunar spinels and chromespinelids have difficulties in displaying the composition of the lunar phases in diagrams (Malysheva, 1980; Haggerty, 1979; Frondel, 1978; Prissel et al., 2014), since there is a clear ions deficiency in octahedral positions in these phases. There is still no typification of lunar chromespinelids yet. The inversion of terrestrial chromespinelids is a well-known fact, whereas divalent iron can be found both in octahedra and in tetrahedra. This might also be the case in lunar spinels. We propose to use the calculations of the crystal-chemical coefficients of lunar chromespinelides as well as of terrestrial ones (Makeyev and Bryanchaninova, 1999; Makeyev, 2013), displaying the results (Table 6) on a triangular prism (Fig. 7), replacing trivalent iron with "reversed" divalent iron (in octahedra). The field of the miscibility gap between the octahedral ions of aluminum and titanium (+$Fe^{2+}_{reverse}$) in the lunar spinelids is much narrower than in the terrestrial phases (Fig. 7). If one day large accumulations of chromium ores of a special composition (*subtitanoalumochromites*) were found on the Moon, they could be successfully used on

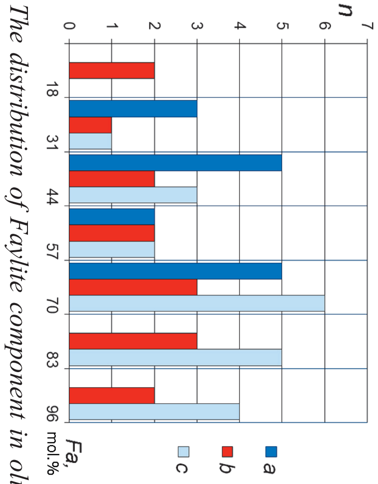

Fig. 5. The distribution of Faylite component in olivine of Lunar regolith. Average values and dispersion of Fayalite compound (Fa, mol.%): a − Luna-16 − 40.8 ± 10.1 (n = 13); b − Luna-20 − 54.6 ± 25.3 (n = 15); c − Luna-24 − Fa = 65.9 ± 19.7 (n = 21)

L-16

Oxides	1	2	3	4	5	6	7	8	9	10	11	12	13
SiO_2	37.38	33.57	36.29	35.33	35.55	37.65	37.43	36.48	34.67	36.44	35.08	37.97	34.24
FeO	27.66	47.75	33.22	38.46	37.41	26.11	27.40	32.56	42.07	32.80	39.19	24.32	43.69
MnO	0.30	0.69	0.45	0.38	0.43	0.42	0.26	0.30	0.44	0.46	0.63	0.10	0.47
MgO	34.01	17.51	29.21	25.08	26.07	35.12	34.19	30.12	22.28	30.00	23.73	36.31	20.02
CaO	0.42	0.48	0.56	0.62	0.54	0.69	0.66	0.45	0.53	0.30	1.36	1.30	1.58
Sum	99.78	100.0	99.73	99.88	100.0	100.0	99.94	99.91	100.0	100.0	100.0	100.0	100.0
Fe^{2+}	0.309	0.595	0.383	0.455	0.440	0.290	0.306	0.373	0.507	0.376	0.467	0.268	0.534
Mn^{2+}	0.003	0.009	0.005	0.005	0.005	0.005	0.003	0.003	0.005	0.005	0.008	0.001	0.006
Mg^{2+}	0.678	0.389	0.600	0.529	0.547	0.695	0.681	0.615	0.479	0.614	0.504	0.713	0.436
Ca^{2+}	0.006	0.008	0.008	0.009	0.008	0.010	0.009	0.007	0.008	0.004	0.021	0.018	0.025

L-20

Oxides	1	2	3	4	5	6	7	8	9	10	11	12	13	14	15
SiO_2	29.86	30.30	35.51	34.91	37.36	32.15	32.24	32.95	33.24	32.16	37.88	34.72	32.89	40.16	40.64
FeO	67.35	64.69	37.25	39.57	28.08	55.49	55.04	51.10	49.69	55.72	25.47	41.90	51.71	13.15	10.81
MnO	0.67	0.95	0.10	0.21	0.38	0.58	0.77	0.57	0.48	0.50	0.09	0.58	0.50	0.10	0.19
MgO	1.32	3.21	25.46	22.44	34.10	11.44	11.85	14.83	16.08	11.54	36.29	22.64	14.66	46.23	48.28
CaO	0.80	0.73	1.64	2.87	0.08	0.29	0.10	0.55	0.41	0.08	0.26	0.16	0.24	0.18	0.09
Sum	100.0	99.88	99.96	100.0	100.0	99.95	100.0	100.0	99.91	100.0	100.0	100.0	100.0	99.93	100.0
Fe^{2+}	0.943	0.893	0.439	0.474	0.314	0.722	0.714	0.648	0.625	0.725	0.281	0.505	0.657	0.137	0.111
Mn^{2+}	0.010	0.013	0.001	0.003	0.004	0.008	0.010	0.007	0.006	0.007	0.001	0.007	0.006	0.001	0.002
Mg^{2+}	0.033	0.079	0.535	0.479	0.680	0.265	0.275	0.335	0.361	0.268	0.714	0.486	0.332	0.857	0.886
Ca^{2+}	0.014	0.013	0.025	0.044	0.001	0.005	0.001	0.009	0.007	0.001	0.004	0.002	0.004	0.002	0.001

L-24

Oxides	1	2	3	4	5	6	7	8	9	10	11	12	13	14	15	16	17	18	19	20	21
SiO_2	30.79	30.37	32.02	31.19	31.25	32.14	32.03	33.03	36.36	33.79	36.85	34.97	35.41	33.08	32.97	32.81	31.84	34.59	36.99	32.50	38.15
FeO	67.53	66.76	65.22	63.97	61.65	59.05	59.23	50.10	33.56	48.06	32.97	44.62	50.64	52.69	52.40	55.47	54.09	45.89	32.13	46.34	22.02
MnO	0.56	0.61	0.52	0.55	0.49	0.44	0.47	0.35	0.25	0.34	0.29	0.33	0.54	0.45	0.41	0.45	0.37	0.32	0.23	0.33	0.24
MgO	0.95	2.02	1.95	4.62	6.58	8.89	8.88	15.11	30.11	18.55	28.25	18.19	11.08	14.16	13.66	11.98	11.78	20.14	31.55	14.84	39.27
CaO	0.53	0.83	1.87	0.63	0.55	0.33	0.33	0.33	0.25	0.36	1.24	1.05	2.02	0.45	0.38	0.22	0.54	0.36	0.24	0.36	0.25
Sum	100.4	100.6	101.6	101.0	100.5	100.8	100.9	98.93	100.5	101.1	99.60	99.16	99.68	100.8	99.82	100.9	98.61	101.3	101.1	94.37	99.92
Fe^{2+}	0.957	0.927	0.910	0.869	0.828	0.779	0.780	0.644	0.378	0.589	0.388	0.566	0.685	0.664	0.674	0.715	0.709	0.556	0.361	0.629	0.238
Mn^{2+}	0.008	0.009	0.007	0.008	0.007	0.006	0.006	0.005	0.003	0.004	0.003	0.004	0.007	0.006	0.005	0.006	0.005	0.004	0.003	0.004	0.003
Mg^{2+}	0.025	0.050	0.049	0.112	0.156	0.209	0.208	0.346	0.616	0.401	0.590	0.413	0.274	0.323	0.314	0.275	0.277	0.434	0.633	0.361	0.756
Ca^{2+}	0.010	0.015	0.033	0.011	0.009	0.006	0.006	0.005	0.004	0.006	0.018	0.017	0.034	0.007	0.006	0.004	0.009	0.006	0.004	0.006	0.003

Table 3. Chemical composition of olivine (wt.%) of lunar regolith and formula coefficients Luna-16 Station, Luna-20 Station, Luna-24 Station. Olivine analyses were performed on the JEOL JXA-8200 device, analyst − A.A. Virus.

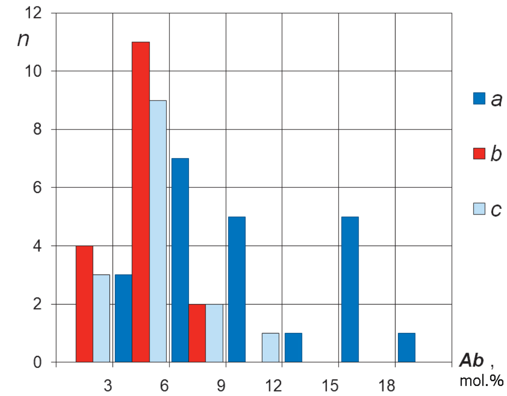

Fig. 6. The distribution of Albite component in plagioclase of Lunar regolith. Average values and dispersion of Albite component (Ab, mol.%): a – Luna-16 – 10.3 ± 4.1 (n = 22); b – Luna-20 – 4.7 ± 2.0 (n = 17); c – Luna-24 – 5.0 ± 2.2 (n = 15)

L-16

Oxides	1	2	3	4	5	6	7	8	9	10	11	12	13	14	15	16	17	18	19	20	21
SiO_2	47.13	45.88	46.56	47.07	49.01	47.85	46.20	42.40	47.92	43.50	45.76	41.41	44.73	47.19	44.09	45.28	43.76	43.15	43.76	45.22	44.78
Al_2O_3	32.80	33.28	32.52	33.52	32.26	31.42	33.96	36.95	33.12	36.89	33.41	37.24	34.84	33.32	35.61	34.70	36.24	36.56	35.49	33.51	34.36
CaO	17.07	15.99	17.10	15.89	15.48	15.41	17.68	20.19	16.46	17.90	17.20	20.27	18.55	17.29	17.90	17.80	18.68	18.24	18.32	17.34	17.12
Na_2O	1.35	2.59	2.32	2.50	2.50	3.12	1.59	0.12	1.86	0.91	1.93	0.87	1.04	1.21	1.73	1.65	1.12	1.40	1.55	2.77	2.79
FeO	1.65	2.26	1.51	1.02	0.75	2.21	0.56	0.33	0.64	0.80	1.71	0.21	0.85	1.00	0.66	0.57	0.21	0.65	0.88	1.15	0.96
Sum	100.0	100.0	100.0	100.0	100.0	100.0	100.0	100.0	100.0	100.0	100.0	100.0	100.0	100.0	100.0	100.0	100.0	100.0	100.0	100.0	100.0
An	91.8	84.5	86.7	84.9	84.6	81.4	90.8	99.3	88.7	94.6	88.8	95.4	94.0	92.7	90.1	90.5	93.7	92.0	91.3	84.7	84.5
Ab	8.2	15.5	13.3	15.1	15.4	18.6	9.2	0.7	11.3	5.4	11.2	4.6	6.0	7.3	9.9	9.5	6.3	8.0	8.7	15.3	15.5

L-20

Oxides	1	2	3	4	5	6	7	8	9	10	11	12	13	14	15	16	17
SiO_2	44.02	44.54	43.18	43.72	44.28	42.83	44.41	44.34	43.87	43.31	43.93	44.02	43.00	42.62	43.01	43.03	45.08
Al_2O_3	34.96	34.74	35.23	35.74	34.80	37.51	34.68	34.84	35.14	36.37	35.37	35.05	36.12	35.30	36.90	36.44	34.07
CaO	19.07	20.51	20.05	19.15	19.49	18.75	19.34	19.21	19.31	19.68	19.17	19.16	18.75	19.44	18.62	18.65	17.85
Na_2O	1.08	0.20	0.07	0.92	0.87	0.90	1.02	1.09	0.86	0.39	0.98	1.02	0.98	0.33	1.07	1.05	2.35
FeO	0.87	0.01	0.72	0.46	0.56	0.01	0.55	0.52	0.82	0.26	0.55	0.75	1.16	0.81	0.40	0.83	0.65
Sum	100.0	100.0	99.28	100.0	100.0	100.0	100.0	100.0	100.0	100.0	100.0	100.0	100.0	98.51	100.0	100.0	100.0
An	94.0	98.9	99.6	94.8	95.2	94.8	94.4	94.0	95.2	97.8	94.5	94.3	94.4	98.1	93.9	94.0	87.0
Ab	6.0	1.1	0.4	5.2	4.8	5.2	5.6	6.0	4.8	2.2	5.5	5.7	5.6	1.9	6.1	6.0	13.0

L-24

Oxides	1	2	3	4	5	6	7	8	9	10	11	12	13	14	15
SiO_2	46.44	46.32	47.91	45.27	45.14	46.24	48.58	44.89	48.11	45.78	46.17	46.59	45.97	46.81	47.02
Al_2O_3	33.02	32.91	32.47	34.12	34.38	33.52	32.13	34.28	31.89	33.25	33.44	32.45	33.01	32.64	30.71
CaO	18.61	18.74	17.41	19.07	18.89	18.73	17.10	19.43	17.63	19.02	18.34	19.18	19.54	19.07	17.78
Na_2O	0.67	0.71	1.51	0.59	0.65	0.88	1.66	0.37	1.30	0.55	0.88	0.67	0.58	0.94	0.98
FeO	1.08	1.11	0.66	0.89	0.88	0.52	0.53	0.93	1.07	1.00	1.17	0.83	0.90	0.54	3.08
Sum	99.82	99.78	99.95	99.94	99.94	99.89	100.0	99.00	100.0	99.61	100.0	99.72	100.0	100.0	99.57
An	96.1	95.9	91.1	96.6	96.2	95.0	90.1	97.9	92.3	96.8	94.9	96.2	96.8	94.7	94.2
Ab	3.9	4.1	8.9	3.4	3.8	5.0	9.9	2.1	7.7	3.2	5.1	3.8	3.2	5.3	5.8

Table 4. Chemical composition of plagioclase (wt.%) of the lunar regolith and minals Luna-16 Station, Luna-20 Station, Luna-24 Station. Analyses were performed on the JSM-5610LV device, analyst – L.O. Magazina.

Oxides	1	2	3	4	5	6	7	8	9	10	11
TiO_2	52.53	52.41	52.91	52.47	52.16	52.61	52.81	52.15	52.78	52.89	53.11
FeO	46.57	46.03	45.99	46.06	43.01	46.36	46.35	46.72	46.11	45.65	46.18
MgO	–	–	–	–	3.15	–	–	–	–	–	–
MnO	0.46	0.43	0.56	0.56	0.42	0.61	0.08	0.50	0.44	0.45	0.49
V_2O_3	0.33	0.25	0.20	0.51	0.28	0.18	0.43	0.18	0.44	0.81	0.14
Cr_2O_3	–	0.69	0.26	0.26	0.51	0.21	0.30	0.38	0.17	–	–
Sum	99.89	99.80	99.92	99.86	99.54	99.96	99.98	99.94	99.94	99.80	99.92
Oxides	**12**	**13**	**14**	**15**	**15**	**17**	**18**	**19**	**20**	**21**	**Average**
TiO_2	52.67	52.97	52.74	52.47	51.72	52.93	52.42	51.2	52.49	52.37	52.51
FeO	46.34	46.45	46.78	46.49	46.74	45.99	46.41	47.48	46.13	46.17	46.19
MgO	–	–	–	–	–	–	–	–	–	–	0.15
MnO	0.42	0.26	0.26	0.31	0.47	0.59	0.56	0.51	0.53	0.36	0.44
V_2O_3	0.44	0.30	0.19	0.19	0.23	0.12	0.14	0.18	0.54	0.46	0.31
Cr_2O_3	–	–	–	0.46	0.70	0.36	0.46	0.61	0.11	0.52	0.29
Sum	99.87	99.98	99.97	99.92	99.87	99.99	99.99	99.98	99.80	99.88	99.89
Oxides	**22**	**23**	**24**	**25**	**26**	**27**	**28**	**29**	**30**	**31**	**Average**
TiO_2	52.74	51.69	52.76	52.62	52.78	52.61	52.67	52.90	52.63	52.65	52.71
FeO	45.82	46.82	46.02	46.62	46.43	46.52	46.43	45.02	46.62	46.63	46.19
MgO	0.76	0.79	0.65	0.24	0.41	0.36	0.41	1.27	0.24	0.28	0.54
MnO	0.32	0.27	0.29	0.32	0.34	0.26	0.34	0.32	0.32	0.26	0.30
Cr_2O_3	0.29	0.29	0.26	0.14	0.12	0.18	0.12	0.46	0.14	0.13	0.21
Sum	99.92	99.86	99.97	99.94	99.96	99.93	99.97	99.97	99.95	99.95	99.95

Table 5. Chemical composition (wt.%) of inclusions ilmenite in regolith basalts Luna-16 (1–21) and Luna-24 (22–31) stations. Ilmenate analyses were performed on the JSM-5610LV device, analyst − L.O. Magazina.

Oxides	L-24											L-20			
	1	2	3	4	5	6	7	8	9	10	11	12	13	14	15
Cr_2O_3	43.56	41.50	41.50	44.01	42.72	40.83	45.04	44.90	43.33	40.90	41.21	44.76	41.13	41.71	43.68
Al_2O_3	14.47	16.64	15.12	17.10	13.12	15.64	17.64	17.68	17.09	11.35	12.95	10.67	18.93	16.76	15.29
TiO_2	2.09	2.18	2.40	1.22	3.14	2.75	1.27	1.24	1.28	6.59	4.69	2.02	1.39	1.58	2.30
V_2O_3	–	–	–	–	–	–	–	–	–	–	–	0.68	0.59	1.19	0.87
FeO_{rev}	6.54	6.95	6.89	5.27	6.86	6.86	4.52	4.51	5.51	7.06	7.85	11.39	5.24	5.78	5.08
FeO	30.29	27.80	32.16	27.25	32.56	31.27	24.61	25.00	28.38	30.93	29.27	23.58	27.03	28.58	27.86
MnO	0.14	0.20	0.12	0.14	0.10	0.16	0.08	0.11	0.11	0.17	0.13	0.00	0.41	0.39	0.29
MgO	2.91	4.73	1.82	5.01	1.51	2.50	6.84	6.56	4.30	2.99	3.91	6.90	5.00	3.89	4.27
Sum	100.00	100.00	100.00	100.00	100.00	100.00	100.00	100.00	100.00	100.00	100.00	100.00	99.72	99.88	99.64
Cr^{3+}	9.251	8.614	8.834	9.163	9.142	8.607	9.232	9.222	9.065	8.490	8.573	9.434	8.493	8.758	9.148
Al^{3+}	4.580	5.147	4.797	5.305	4.183	4.913	5.389	5.411	5.327	3.512	4.015	3.351	5.825	5.244	4.772
Ti^{4+}	0.845	0.863	0.971	0.485	1.277	1.102	0.494	0.483	0.509	2.602	1.857	0.808	0.547	0.632	0.914
V^{3+}	–	–	–	–	–	–	–	–	–	–	–	0.120	0.101	0.209	0.152
Fe^{2+}_{rev}	1.323	1.374	1.396	1.045	1.397	1.376	0.882	0.881	1.097	1.395	1.554	2.285	1.031	1.156	1.012
Fe^{2+}	6.804	6.105	7.242	6.002	7.369	6.972	5.336	5.432	6.278	6.791	6.440	5.258	5.905	6.347	6.172
Mn^{2+}	0.031	0.044	0.027	0.030	0.023	0.035	0.018	0.025	0.025	0.038	0.028	0.000	0.090	0.088	0.064
Mg^{2+}	1.165	1.852	0.731	1.968	0.609	0.993	2.646	2.543	1.697	1.171	1.532	2.742	1.946	1.539	1.687
Subtype	*Subtitanoalumochromite*									*Subtitano-subalumochromite*			*Subtitano-alumochromite*		

Table 6. Chemical composition (wt.%) of lunar regolith chromespinelides and formula coefficients. The chemical composition of lunar chromespinelides was recalculated taking into account the inversion of the crystal lattice and the occurrence of a part of divalent iron in octahedral positions. The accuracy of the analysis meets the standards − 0.01 abs.%, the sum of the determined components is not worse than 99%. In some samples, the content of vanadium in chromespinelides was not determined, so there is a dash in the table. Analyses of chromespinelides are made on the JEOL JXA-8200 device, analyst − A.A. Virus.

an industrial scale in metallurgical processing for the production of ferrochrome.

Different to the Earth's mineral world, no hydroxyl, or water-containing minerals have been found on the Moon so far, except for isolated discoveries of water-containing glasses (Saal et al., 2008) and possibly olivine dehydrogenation (Khisina et al., 2013). Possibly, they decomposed in the process of prolonged degassing and the absence of an atmosphere on the Moon, but most likely they did not form at all.

Geochemical features of the lunar regolith

It is known that the most common elements in the material composition of rocks and minerals of the

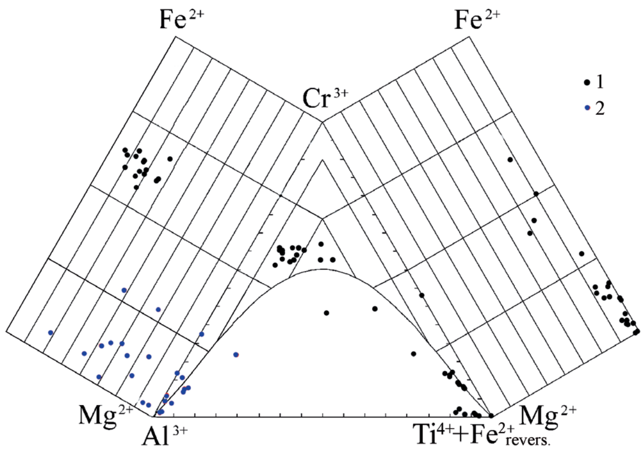

Fig. 7. Diagram of the composition of lunar chromespinelids. 1 − Luna -24 (Table. 6); 2 − alumochromespinelides and pink spinels, recalculated analyses (Frondel, 1978)

Moon are: silicon, oxygen, aluminum, iron, calcium, magnesium, titanium, sodium; very little quantities chromium, manganese, nickel, potassium, sulfur, phosphorus; almost none volatile, carbon, chlorine. The remaining elements are present only in micro-quantities.

Discussion of the results

Since there is an element of randomness in the selection of the objects of study – lunar regolith particles, even a limited number of analyses can be used in statistical generalizations to compare regional features of regolith in different landing sites of automatic lunar stations (Luna-16, -20, -24). Comparing the prevalence of lunar minerals (Table. 1) and typochemical features of rock-forming and accessory minerals (Tables 2–6, Fig. 4–7), the following should be noted:

– the iron content of the rock-forming clinopyroxene is significantly higher in marine olivine basalts (Table 2, Fig. 4), *hedenbergite* and pyroxferroite are the most widespread in them, orthopyroxene-*bronzite*, on the contrary, is present only among continental rocks, probably originating from norites, gabbro-norites, lherzolites;

– iron content of the lunar olivine varies in a very wide range of forsterite with Fa from 11.5 mol.% to fayalite with Fa 95.0 mol.% (Table 3, Fig. 5), this demonstrated a high diversity of olivine in the continental part of the moon. In the Mare Fecunditatis, olivine is the least ferruginous (probably from olivine basalt), and in Mare Crisium, on the contrary, it is the most ferruginous. It can be assumed that olivine mixes into the regolith from several types of rocks, as demonstrated by its bimodal distribution;

– the basicity of plagioclase also varies widely from anorthite with 0.4 mol.% Ab to bitovnit with 18.5 mol.% Ab (Table 4, Fig. 6), the distribution being bimodal as well. The regolith of all the stations contains the most basic plagioclase, which is inherent in the anorthosite rock on the Earth. Plagioclase from Mare Fecunditatis is represented by both anorthite and bitovnite, the latter is found in lunar rocks – olivine basalt and gabbro;

– ilmenite (Table 5) is most common in the basalts of the lunar seas;

– chrome ulvospinel and *subtitanoalumochromite* are most common for the continental part of the Moon;

– in the basalts of the lunar seas, iron sulfides are most common – troilite and pyrrhotite.

A group of reserachers from IGEM research insitute (Mokhov, Kartashov, Bogatikov, 2007) have discovered, native metal films microdissociations of several types (including iron group metals) on the surface of lunar regolith particles. Those and their exotic alloys coincide in composition with syngenetic native metals films (Makeyev, Kriulina, 2012) on mantle diamonds from several deposits of Russia and of the world. This observation may also indicate a reducing medium for mineral formation.

Conclusion

The existance of lunar mineral resources has always motivated reserachers for a more detailed study of the Earth's satellite. In anticipation of new manned missions to the Moon, it is tempting to make an assumption about the most likely discoveries of near-surface mineral deposits anagolue to the distribution of minerals in the earth's rocks. We recon the most likely findings to be titanium occurrences in the form of ilmenite in basalts and olivine basalts of the lunar seas; chromium and iron ores in anorthosite lopolites (similar to Bushveld) and in "Mg-suite" rocks (Prissel et al., 2014) with possible native Pt-Pd and Pt-Fe mineralization. Since vast areas of the lunar seas are covered with basalt outpourings that are very similar to Siberian traps, they can be specialized for interspersed copper-nickel sulfide ores (Krivolutskaya, Bryanchaninova, 2011). In lunar mantle rocks (dunites, lherzolites), diamonds may be present on the reverse side. Noteworthy, the geodynamic histories of the Earth and the Moon are radically different, thus, the patterns of formation and placement of mineral depositions will also differ significantly.

Acknowledgments

The authors are grateful to A.A. Viryus and L.O. Magazina for their help in analytical research and to the reviewers for helpful discussion of the work.

References

Barsukov V.L. (1977). Preliminary data for the regolith core brought to Earth by the automatic lunar station Luna 24. *Proc. 8th Moon Sci. Conf.*, pp. 3303–3318. (In Russ.)

Bell P.M., Mao H.K., Hazen R.M. and Mao A.L. (1978). Luna 24 sample from Mare Crisium: New structural features in lunar glasses from the study of crystal-field spectra. In: *Mare Crisium: The view from Luna 24*. Eds. Merrill R.B. and Papike J.J. N.Y.: Pergamon Press, pp. 265–280.

Bogatikov O.A. (1979). Anortozity [Anorthosites]. Moscow: Nauka, 232 p. (In Russ.)

Bogatikov O.A., Makeyev A.B. (2012). Features of the Mineralogy of the Lunar regolith, Luna-24. *Proc. 13 Int. Conf.: Physical-chemical and petrophysical research in Earth Sciences*. Moscow, pp. 39–42. (In Russ.).

Frondel J.W. (1978). Mineralogiya Luny [Lunar Mineralogy]. Moscow: Mir, 333 pp. (In Russ.)

Haggerty S.E. (1979). Moon-20: chemistry of minerals – spinel, pleonast, chromite, ulvoshpinel, ilmenite and rutile. Soil from the mainland region of the moon. Moscow: Nauka, pp. 267–277. (In Russ.)

Khisina N.R. (1987). Subsolidus transformations of solid solutions of rock-forming minerals. Moscow: Nauka. 207 pp. (In Russ.)

Khisina N.R., Makarov E.S. (1977). Cation distribution and exsolution in the Luna-20 pyroxenes as the chronological indicator of their termal history. *Earth, Moon, and Planets*, 17(2), pp. 149–165. https://doi.org/10.1007/BF00640905

Khisina N.R., Wirth R., Abart R., Rhede D., Heinrich W. (2013). Oriented chromite-diopside symplectic inclusions in olivine from lunar regolith delivered by "Luna-24". *Geochimica et Cosmochimica Acta*, 104, pp. 84–98. https://doi.org/10.1016/j.gca.2012.10.050

Krivolutskaya N.A., Bryanchaninova N.I. (2011). Olivines of Igneous Rocks. *Russian Journal of General Chemistry*, 81(6), pp. 1302–1314. https://doi.org/10.1134/S1070363211060363

Lunar soil from Mare Crisium [Lunnyi grunt iz morya Krizisov]. (1980). Moskow: Nauka, 360 pp. (In Russ.)

Magmatism of the Earth and the Moon: Experience of comparative analysis [Magmatizm Zemli i Luny: opyt sravnitelnogo analiza]. (1990). Moscow: Nauka, 211 pp. (In Russ.)

Makeyev A.B. (2006). Typomorphic features of Cr-spinals and mineralogical prospecting guides for Cr ore mineralization. *Russian Journal of Earth Sciences*, 8(3), pp. 1–19. http://dx.doi.org /10.2205/2006ES000196

Makeyev A.B. (2013). Lunar chromespinelids from the regolith of Luna-16, -20, -24. *Modern problems of theoretical, experimental and applied Mineralogy (Yushkin readings–2013): Proc. Mineralogical Seminar*. Syktyvkar: Institute of Geology, Komi science center UB RAS, pp. 97–99. (In Russ.)

Makeyev A.B., Bryanchaninova N.I. (1999). Topomineralogiya ultrabazitov Polyarnogo Urala [Typomineralogy of Ultrabasites of the Polar Urals]. St. Petersburg: Nauka, 252 p. (In Russ.)

Makeyev A.B., Bryanchaninova N.I. (2012). Mineral composition of basalts of the Volsko–Vymskaya ridge (Middle Timan). *Crystalline and solid non-crystalline state of mineral matter: Proc. Mineralogical Seminar*. Syktyvkar: Geoprint, pp. 281–283. (In Russ.)

Makeyev A.B., Kriulina G.Yu. (2012). Metal Films on the Surface and within Diamond Crystals from Arhangelskaya and Yakutian Diamond Provinces. *Geology of Ore Deposits*, 54(8), pp. 663–673. https://doi.org/10.1134/S1075701512080107

Makeyev A.B., Lutoev V.P., Vtorov I.P., Braynchaninova N.I., Makavetskas A.R. (2020). Composition and spectroscopy of olivine xenocrysts from the Hawaiian tholeiitic basalts. *Uchenye Zapiski Kazanskogo Universiteta. Seriya Estestvennye Nauki*, 162(2), pp. 253–273. https://doi.org/10.26907/2542-064X.2020.2.253-273 (In Russ.)

Malysheva T.V. (1980). NGR-spectroscopy of regolith samples from Mare Crisium. *Lunar soil from Mare Crisium.* Moscow: Nauka, pp. 300–308. (In Russ.)

Mokhov A.V., Kartashov P.M., Bogatikov O.A. (2007). Luna pod mikroskopom: novye dannye po mineralogii Luny: Atlas [The Moon under the microscope: new data on the moon's Mineralogy: Atlas]. Moscow: Nauka, 127 pp. (In Russ.)

Regolith from the highland region of the Moon [Grunt iz materikovogo raiona Luny]. (1979). Moscow: Nauka, 708 pp. (In Russ.)

Prissel T.C., Parman S.W., Jackson C.R.M., et al. (2014). Pink Moon: The petrogenesis of pink spinel anorthosites and implications concerning Mg-suite magmatism. *Earth and Planetary Science Letters*, 403, pp. 144–156. https://doi.org/10.1016/j.epsl.2014.06.027

Saal A.E., Haur E.H., Lo Cascio M., Van Orman J.A., Rutherford M.J. and Cooper R.F. (2008). The Volatile Content of the Lunar Volcanic Glasses: Evidence for the Presence of Water in the Moon's Interior. *Nature*, 454, pp. 192–195. https://doi.org/10.1038/nature07047

Taylor G.J., Warner R.D. and Keil K. (1978). VLT mare basalts: Impact mixing, parent magma types, and petrogenesis. In: *Mare Crisium: The view from Luna 24*. Eds. Merrill R.B. and Papike J.J. Pp. 357–370.

The Moon – A new appraisal from space missions and laboratory analyses (1977). London: The Royal Society, 606 p.

About the Authors

Alexander B. Makeyev – Dr. Sci. (Geology and Mineralogy), Professor, Leading Researcher, Laboratory of Ore Deposits Geology, Institute of Ore Geology, Petrography, Mineralogy and Geochemistry of the Russian Academy of Sciences

35, Staromonetny Lane, Moscow, 119017, Russian Federation

e-mail: abmakeev@igem.ru

Nataliya I. Bryanchaninova – Dr. Sci. (Geology and Mineralogy), Leading Researcher, Geological Institute of the Russian Academy of Sciences

7, Pyzhevsky lane, Moscow, 119017, Russian Federation

Manuscript received 22 January 2021;
Accepted 12 March 2021; Published 30 March 2021